Satyanarayana G. Manyam
Infoscitex Corporation,
DCS Company,
Dayton, OH 45431
e-mail: msngupta@gmail.com

Sivakumar Rathinam
Department of Mechanical Engineering,
Texas A&M University,
College Station, TX 77843
e-mail: srathinam@tamu.edu

On Tightly Bounding the Dubins Traveling Salesman's Optimum

The Dubins traveling salesman problem (DTSP) has generated significant interest over the last decade due to its occurrence in several civil and military surveillance applications. This problem requires finding a curvature constrained shortest path for a vehicle visiting a set of target locations. Currently, there is no algorithm that can find an optimal solution to the DTSP. In addition, relaxing the motion constraints and solving the resulting Euclidean traveling salesman problem (ETSP) provide the only lower bound available for the DTSP. However, in many problem instances, the lower bound computed by solving the ETSP is far below the cost of the feasible solutions obtained by some well-known algorithms for the DTSP. This paper addresses this fundamental issue and presents the first systematic procedure for developing tight lower bounds for the DTSP.
[DOI: 10.1115/1.4039099]

1 Introduction

Given a set of targets on a plane, an unmanned vehicle, and its minimum turning radius (ρ), the Dubins traveling salesman problem (DTSP) aims to find a path for the vehicle such that each target is visited at least once, the radius of curvature of any point in the path is at least equal to ρ, and the length of the path is minimal. This problem is a generalization of the Euclidean traveling salesman problem (ETSP) and is NP-hard [1,2]. The DTSP belongs to a class of task allocation and path planning problems envisioned for an unmanned aerial vehicle in Ref. [3]. The DTSP has received significant attention in the literature [1,2,4–16], mainly due to its importance in unmanned vehicle applications, the simplicity of the problem statement, and its status as a hard problem to solve because it inherits features from both optimal control and combinatorial optimization.

A feasible path (or a feasible solution) to the DTSP is a curvature constrained path where the radius of curvature at any point in the path is at least equal to ρ and each target is visited at least once. The cost of a path is defined by its length. The optimal cost of the DTSP is the length of a shortest feasible path for the DTSP. Any feasible path whose length is equal to the optimal cost is an optimal solution to the DTSP. There is currently no algorithm in the literature that can find an optimal solution to the DTSP. Heuristics and approximation algorithms have been developed over the last decade to find feasible solutions for the DTSP. Tang and Ozguner [11] presented gradient-based heuristics for both single and multiple vehicle variants of the DTSP. Savla et al. [12] used an optimal solution to the ETSP to find a feasible solution for the DTSP, and they bound the cost of the feasible solution with respect to the optimal cost of the ETSP. Rathinam et al. [1] developed an approximation algorithm for the DTSP in cases where the distance between any two targets is at least equal to 2ρ. Le Ny et al. [2] developed an approximation algorithm for the DTSP in which the approximation guarantee is inversely proportional to the minimum distance between any two targets. The weakness of the approximation guarantees of these algorithms for the DTSP is due to the lack of a good lower bound, as all these algorithms essentially use the Euclidean distances between the targets to bound the cost of a feasible solution.

Contributed by the Dynamic Systems Division of ASME for publication in the Journal of Dynamic Systems, Measurement, and Control. Manuscript received February 10, 2016; final manuscript received January 22, 2018; published online March 7, 2018. Assoc. Editor: Azim Eskandarian.

Other heuristics have been used for solving the DTSP. A receding horizon approach that involves finding an optimal path through three consecutive targets is used to generate feasible solutions in Ref. [14]. The heuristic in Ref. [4] finds a feasible solution by minimizing the sum of the distances traveled by the vehicle and the sum of the changes in the heading angles at each of the targets. Macharet et al. [5,7] first obtain a tour by solving the ETSP and then select the heading angle at each target using an orientation-assignment heuristic. A multiple lookahead approach is used to find feasible solutions in Refs. [8] and [17]. Metaheuristics have also been developed to find feasible solutions for the DTSP in Refs. [9] and [10].

Another common approach [13,18] involves discretizing the heading angle at each target and posing the resulting problem as a one-in-a-set TSP (Fig. 1). The greater the number of discretizations, the closer an optimal one-in-a-set TSP solution gets to the optimal DTSP solution. This approach provides a natural way to find a good, feasible solution to the problem [18]. However, this also requires us to solve a large one-in-a-set TSP, which is combinatorially hard. Nevertheless, this approach provides an upper bound [13] for the optimal cost of the DTSP, and simulation results indicate that the cost of the solutions starts to converge with more than 15 discretizations at each target.

The fundamental question with regard to all the above heuristics and approximation algorithms is how close a feasible solution *actually is* to the optimum. For example, Fig. 2 shows the cost of the feasible solutions obtained by solving the one-in-a-set TSP and the ETSP for 25 instances with 20 targets in each instance. Even with 32 discretizations of the possible angles at each target, the cost of the feasible solution is at least 30% greater than the corresponding optimal ETSP cost for several of these instances. As there is currently no systematic procedure available to find the optimal cost for the DTSP, identifying a tight lower bound is crucial for determining the quality of the solutions that have been provided as well as for developing constant factor approximation algorithms.

This fundamental question was the motivation for the bounding algorithms in Refs. [19–22]. In these algorithms, the requirement that the arrival and departure angles must be equal at each target is removed, and instead there is a penalty in the objective function whenever the requirement is violated. This results in a max–min problem where the minimization problem is an asymmetric TSP (ATSP), and the cost of traveling between any two targets requires solving a new optimal control problem. In terms of lower bounding, the difficulty with this approach is that we are not currently

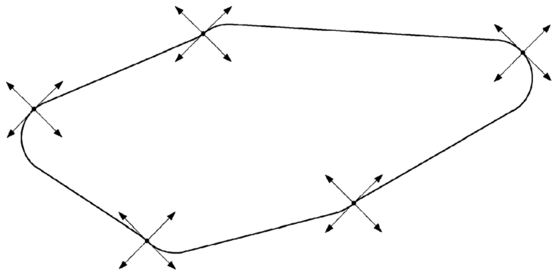

Fig. 1 There are four possible headings at each target. A feasible solution for the DTSP can be obtained by choosing a heading at each target and finding a corresponding optimal TSP path.

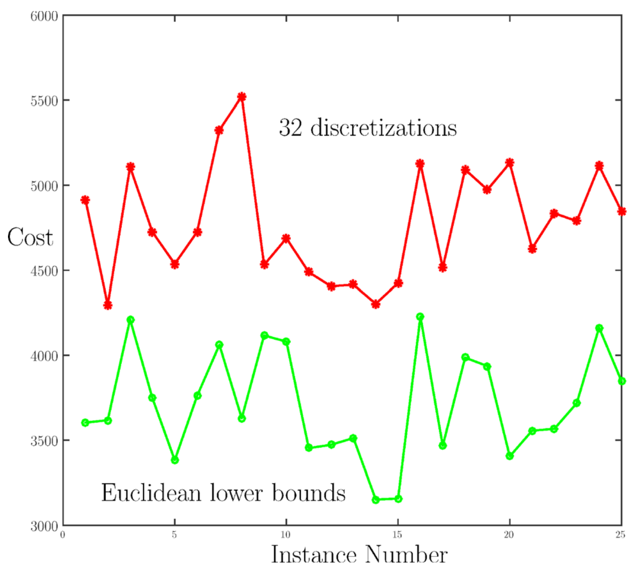

Fig. 2 A comparison between the cost of the feasible solution (upper bound) obtained by solving the one-in-a-set TSP with 32 discretizations and the optimal cost of the corresponding ETSP (lower bound) for 25 instances. There are 20 targets in each instance, and the location of each target is uniformly sampled from a 1000 × 1000 square. Also, the minimum turning radius of the vehicle is set to 100.

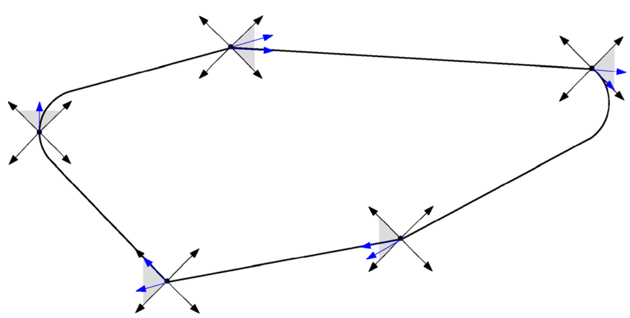

Fig. 3 There are four intervals at each target. A lower bound for the DTSP can be obtained by choosing an interval and restricting both the arrival and the departure angles to be in the chosen interval at each target and then finding a corresponding optimal TSP path. The shaded interval at each target shows the chosen interval with the arrival and departure angles.

aware of any algorithm that will guarantee a lower bound for the optimal control problem. Nonetheless, this is a useful approach, and advances in lower bounding optimal control problems will lead to finding lower bounds for the DTSP.

In this paper, we propose a new approach for finding tight lower bounds for the DTSP. This is the first systematic procedure available for the DTSP and is a natural counterpart to the one-in-a-set TSP approach we discussed earlier. In this approach, we remove the requirement that the arrival angle and the departure angle at each target must be the same, but we restrain these angles so that they belong to one sector or interval (refer to Fig. 3). The lower bounding problem (BP) aims to choose an interval at each target such that the arrival angle and the departure angle at the target belong to the same interval, each target is visited at least once, and the sum of the costs of traveling between the targets is minimized. The cost of traveling between two intervals corresponding to two distinct targets now reduces to a new optimal control problem, which we refer to as the *Dubins interval problem*. Given two targets and an interval at each target, the problem is to find a feasible path such that the departure angle at the initial target and the arrival angle at the final target belong to the given intervals and the length of the path is minimal. The lower bounding problem is a one-in-a-set TSP and can be solved just like the upper bounding problem. If the size of each of the intervals at each target reduces to zero, the lower bounding problem reduces to the DTSP. If there is only one interval of size 2π at each target, the result is a Euclidean TSP. As the size of the intervals at the targets becomes smaller, the one-in-a-set TSP becomes combinatorially hard, similar to the upper bounding problem. Nevertheless, this provides a systematic approach for finding lower bounds for the DTSP, provided the Dubins interval problem can be solved.

The Dubins interval problem is a new generalization of the standard Dubins problem [23] which has not been formulated or solved[1] in the literature. The difficulty with solving this problem lies in the fact that the length of the shortest feasible paths between any two targets is a nonlinear, discontinuous function of the heading angles of the targets. Therefore, finding the optimal heading angles from the given intervals at the targets that minimizes the length of the path is nontrivial. In this paper, we solve the interval problem using the monotonicity properties and the extremal values of the length of the feasible paths.

The first main contribution of this paper is in formulating the lower bounding problem for the DTSP as a novel one-in-a-set TSP where the cost of traveling between any two targets requires solving a Dubins interval problem. This is the first formulation that aims to provide a tight lower bound for the DTSP. The second main contribution is in formulating the Dubins interval problem and providing an algorithm to solve this problem by exploiting its structure and monotonicity properties. Numerical results are then presented to corroborate the performance of the proposed lower bounding approach for 25 instances each involving 10, 15, and 20 targets.

This paper is organized as follows: The lower bounding problem is formulated in Sec. 2. Dubins interval problem is formally stated in Sec. 3. Results on the structure and properties of an optimal path for the Dubins interval problem are shown in Sec. 4. Algorithms are presented in Sec. 5 for solving the main parts of the Dubins interval problem. The simulations results are then presented in Sec. 6. Section 7 concludes the paper.

2 Lower Bounding Problem Formulation

The set of targets is denoted by $T = \{1, 2, \ldots, n\}$, where n is the number of targets. The set of available angles $[0, 2\pi]$ at any target i is partitioned into a collection of closed intervals denoted by $\mathcal{I}_i := \{[0, \varphi_{i1}], [\varphi_{i1}, \varphi_{i2}], \ldots, [\varphi_{im_{i-1}}, \varphi_{im_i} = 2\pi]\}$, where $m_i (\geq 1)$ denotes the number of intervals at target i and the φ_{ij} are constants

[1]We point out that there is also another approach based on optimal control in Ref. [24]. However, the approach in Ref. [24] still relies on the results of this paper. Second, unlike the analysis and results in this paper, the work in Ref. [24] does not provide information about the rate of change of lengths of the paths as a function of the heading angles at the targets. This information is critical and very useful in the development of bounds for the feasible solutions and approximation algorithms for the DTSP.

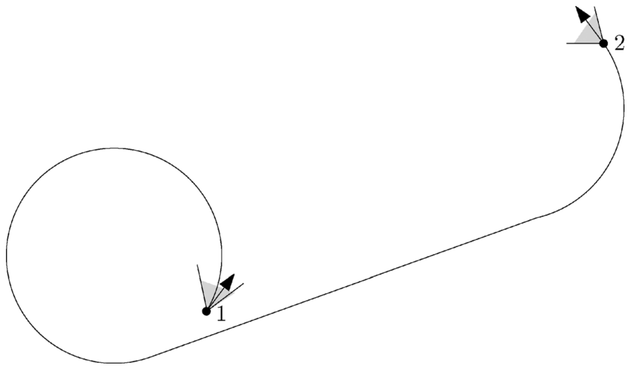

Fig. 4 A feasible solution to the Dubins interval problem

such that $0 \leq \varphi_{i1} \leq \varphi_{i2} \leq \cdots \leq \varphi_{im_i} = 2\pi$. Let (x_i, y_i) denote the location of target $i \in T$, and let the arrival angle and the departure angle of the vehicle at target i be denoted by θ_{ia} and θ_{id}, respectively. The configuration of the vehicle leaving target i at θ_{id} is then denoted by (x_i, y_i, θ_{id}), and (x_i, y_i, θ_{ia}) similarly denotes the vehicle's arrival configuration. The length of the shortest Dubins path from (x_i, y_i, θ_{id}) to (x_j, y_j, θ_{ja}) is denoted by $d_{ij}(\theta_{id}, \theta_{ja})$. Given an interval I_i at target i and an interval I_j at target j, define $d^*_{ij}(I_i, I_j) := \min_{\theta_{id}\in I_i, \theta_{ja}\in I_j} d_{ij}(\theta_{id}, \theta_{ja})$. The objective of the BP is to find a sequence of targets $(s_1, s_2, \ldots, s_n)$, $s_i \in T$, to visit and an interval $I_{s_i} \in \mathcal{I}_i$ for each target $s_i \in T$ such that

- each target is visited at least once, and
- the cost $\sum_{i=1}^{n-1} d^*_{s_i s_{i+1}}(I_{s_i}, I_{s_{i+1}}) + d^*_{s_n s_1}(I_{s_n}, I_{s_1})$ is minimized.

Addressing this BP first requires solving $\min_{\theta_{id}\in I_i, \theta_{ja}\in I_j} d_{ij}(\theta_{id}, \theta_{ja})$. Once this problem is solved, the BP is essentially a one-in-a-set TSP. In this paper, we transform the one-in-a-set TSP into an ATSP using the Noon-Bean transformation [25] and then convert the resulting ATSP into a symmetric TSP using the transformation in Ref. [26]. The symmetric TSP is solved using the Concorde[2] solver [27] to find an optimal solution. This approach is already well known and is discussed in detail in Ref. [18]. Therefore, we focus on solving the Dubins interval problem in Sec. 3. Prior to that, we first formally state the lower bounding result in the following proposition.

Proposition 2.1. *The optimal cost to the BP is a lower bound to the DTSP*.

Proof. Consider an optimal path to the DTSP. Suppose the heading angle of a vehicle traveling this path at target i belongs to interval I_i. Let the vehicle travel to target j after i in the optimal path. Clearly, the length of the optimal path from target i to target j must be at least equal to $d^*_{ij}(I_i, I_j)$. Also, the intervals at the targets and the sequence of targets corresponding to the optimal path are feasible solutions to the BP. Therefore, the cost of the optimal path to the DTSP must be at least equal to the optimal cost of the BP. Hence proved. □

3 Dubins Interval Problem

Without loss of generality, let the Dubins interval problem be denoted as $\min_{\theta_1\in I_1, \theta_2\in I_2} d_{12}(\theta_1, \theta_2)$, where $d_{12}(\theta_1, \theta_2)$ indicates the shortest path (also referred to as the Dubins path) for traveling from (x_1, y_1, θ_1) to (x_2, y_2, θ_2) subject to the minimum turning radius constraint (Fig. 4). Here the interval I_k is defined as $[\theta_k^{\min}, \theta_k^{\max}] \subseteq [0, 2\pi]$ for $k = 1, 2$. Given an initial configuration (x_1, y_1, θ_1) and a final configuration (x_2, y_2, θ_2), Dubins [23] showed that the shortest path for a vehicle to travel between the two configurations subject to the minimum turning radius (ρ) constraint must consist of at most three segments, where each segment is a circle of radius ρ or a straight line. Specifically, if a curved segment of radius ρ along which the vehicle travels in a counterclockwise (clockwise) rotational motion is denoted by $L(R)$, and the segment along which the vehicle travels straight is denoted by S, then the shortest path is one of RSR, RSL, LSR, LSL, RLR, and LRL.

Let $\mathrm{RSL}(\theta_1, \theta_2)$ denote the length of the RSL path from (x_1, y_1, θ_1) to (x_2, y_2, θ_2). $\mathrm{RSL}(\theta_1, \theta_2)$ is set to ∞ if the RSL path does not exist. Let $\mathrm{RSR}(\theta_1, \theta_2)$, $\mathrm{LSR}(\theta_1, \theta_2)$, $\mathrm{LSL}(\theta_1, \theta_2)$, $\mathrm{RLR}(\theta_1, \theta_2)$, and $\mathrm{LRL}(\theta_1, \theta_2)$ be defined in a similar way. Using these definitions, the Dubins interval problem can be written as follows:

$$\begin{aligned}
&\min_{\theta_1\in I_1, \theta_2\in I_2} d_{12}(\theta_1, \theta_2) \\
&= \min_{\theta_1\in I_1, \theta_2\in I_2} \{\mathrm{RSR}(\theta_1, \theta_2), \mathrm{RSL}(\theta_1, \theta_2), \mathrm{LSR}(\theta_1, \theta_2), \\
&\qquad \mathrm{LSL}(\theta_1, \theta_2), \mathrm{RLR}(\theta_1, \theta_2), \mathrm{LRL}(\theta_1, \theta_2)\} \qquad (1)
\end{aligned}$$

Remark 3.1. $d_{12}(\theta_1, \theta_2)$ is a lower semicontinuous function and is minimized over closed and bounded intervals I_1 and I_2. Therefore, the Dubins interval problem is well defined, i.e., there exist $\theta_1^* \in I_1$ and $\theta_2^* \in I_2$ such that $d_{12}(\theta_1^*, \theta_2^*) = \min_{\theta_1\in I_1, \theta_2\in I_2} d_{12}(\theta_1, \theta_2)$.

To solve the Dubins interval problem, we also consider shortest paths that contain at most two segments between (x_1, y_1) and (x_2, y_2). For any path $\mathcal{T} \in \{\mathrm{RS}, \mathrm{LS}, \mathrm{SR}, \mathrm{SL}, \mathrm{RL}, \mathrm{LR}\}$ and $\theta_1 \in I_1$, let $\mathcal{T}^1(\theta_1)$ denote the distance of the shortest path of type $\mathcal{T}$ that starts at (x_1, y_1) with a departure angle of θ_1 and arrives at (x_2, y_2) with an arrival angle in I_2. In this case, the arrival angle at (x_2, y_2) will be a function of θ_1 and $\mathcal{T}$ and is denoted as $\theta_2(\mathcal{T}, \theta_1)$. $\mathcal{T}^1(\theta_1)$ is set to ∞ if a path of type $\mathcal{T}$ does not exist. Similarly, let $\mathcal{T}^2(\theta_2)$ denote the distance of the shortest path of type $\mathcal{T}$ that starts at (x_1, y_1) with a departure angle in I_1 and arrives at (x_2, y_2) with an arrival angle of θ_2. In this case, the departure angle at (x_1, y_1) will be a function of θ_2 and $\mathcal{T}$ and is denoted as $\theta_1(\mathcal{T}, \theta_2)$. $\mathcal{T}^2(\theta_2)$ is set to ∞ if the path of type $\mathcal{T}$ does not exist. From the definitions, note that $\min_{\theta_1\in I_1} \mathcal{T}^1(\theta_1) = \min_{\theta_2\in I_2} \mathcal{T}^2(\theta_2)$.

In Sec. 4, we will first show how to simplify $\min_{\theta_1\in I_1, \theta_2\in I_2} \mathcal{P}(\theta_1, \theta_2)$ for any path $\mathcal{P} \in \{\mathrm{RSR}, \mathrm{RSL}, \mathrm{LSR}, \mathrm{LSL}\}$. Then we will address the LRL and the RLR paths. These results will then be combined to develop an algorithm for the Dubins interval problem stated in Eq. (1). We will show that an optimal path to the Dubins interval problem must be one of the following:

(1) an optimal path consisting of at most three segments such that both the arrival and departure angles at each target belong to one of the boundary values of the respective intervals, or
(2) an optimal path consisting of at most two segments such that the angle constraints are satisfied.

4 Structural Properties of an Optimal Path for the Dubins Interval Problem

4.1 Optimizing RSR, RSL, LSR, and LSL Paths. The following result is known [28] for each of the paths $\mathcal{P} \in \{\mathrm{RSR}, \mathrm{RSL}, \mathrm{LSR}, \mathrm{LSL}\}$ from (x_1, y_1, θ_1) to (x_2, y_2, θ_2):

Lemma 4.1. *For any* $\mathcal{P} \in \{\mathrm{RSR}, \mathrm{RSL}, \mathrm{LSR}, \mathrm{LSL}\}$ *and* $i = 1, 2$, *either* $(\partial\mathcal{P}(\theta_1, \theta_2)/\partial\theta_i) \geq 0\,\forall\,\theta_i$ *or* $(\partial\mathcal{P}(\theta_1, \theta_2)/\partial\theta_i) \leq 0\,\forall\,\theta_i$ *when* $\mathcal{P}$ *exists and none of its curved segments vanishes.*

Now let us apply the above lemma to the RSL path. The RSL path ceases to exist when the segment S vanishes, i.e., the RSL path reduces to an RL path. In addition, when one of the curved segments vanishes, the RSL path reduces to either the RS or the SL path (refer to Fig. 5). Therefore, given θ_1, the optimum for $\min_{\theta_2\in[\theta_2^{\min}, \theta_2^{\max}]} \mathrm{RSL}(\theta_1, \theta_2)$ must be attained when $\theta_2 = \theta_2^{\min}$ or

[2]Concorde is a computer code available for academic research used for solving the symmetric TSP and related network optimization problems.

$\theta_2 = \theta_2^{\max}$ or when the RSL path reduces to an RL, RS, or SL path. This can be stated as follows:

$$\min_{\theta_2\in I_2}\{\mathrm{RSL}(\theta_1,\theta_2)\} := \min\{\mathrm{RSL}(\theta_1,\theta_2^{\min}),\mathrm{RSL}(\theta_1,\theta_2^{\max}),\mathrm{RS}^1(\theta_1),\mathrm{SL}^1(\theta_1),\mathrm{RL}^1(\theta_1)\} \tag{2}$$

Therefore,

$$\begin{aligned}\min_{\theta_1\in I_1}\min_{\theta_2\in I_2}\{\mathrm{RSL}(\theta_1,\theta_2)\} &= \min_{\theta_1\in I_1}\min\{\mathrm{RSL}(\theta_1,\theta_2^{\min}),\mathrm{RSL}(\theta_1,\theta_2^{\max}),\mathrm{RS}^1(\theta_1),\\ &\quad \mathrm{SL}^1(\theta_1),\mathrm{RL}^1(\theta_1)\}\\ &= \min\{\min_{\theta_1\in I_1}\mathrm{RSL}(\theta_1,\theta_2^{\min}),\min_{\theta_1\in I_1}\mathrm{RSL}(\theta_1,\theta_2^{\max}),\\ &\quad \min_{\theta_1\in I_1}\{\mathrm{RS}^1(\theta_1),\mathrm{SL}^1(\theta_1),\mathrm{RL}^1(\theta_1)\}\}\end{aligned} \tag{3}$$

Similarly, using Lemma 4.1 again, we get the following:

$$\begin{aligned}\min_{\theta_1\in I_1}\mathrm{RSL}(\theta_1,\theta_2^{\min}) &= \min\{\mathrm{RSL}(\theta_1^{\min},\theta_2^{\min}),\mathrm{RSL}(\theta_1^{\max},\theta_2^{\min}),\mathrm{RS}^2(\theta_2^{\min}),\\ &\quad \mathrm{SL}^2(\theta_2^{\min}),\mathrm{RL}^2(\theta_2^{\min})\}\end{aligned} \tag{4}$$

$$\begin{aligned}\min_{\theta_1\in I_1}\mathrm{RSL}(\theta_1,\theta_2^{\max}) &= \min\{\mathrm{RSL}(\theta_1^{\min},\theta_2^{\max}),\mathrm{RSL}(\theta_1^{\max},\theta_2^{\max}),\mathrm{RS}^2(\theta_2^{\max}),\\ &\quad \mathrm{SL}^2(\theta_2^{\max}),\mathrm{RL}^2(\theta_2^{\max})\}\end{aligned} \tag{5}$$

Now, one can easily verify the following:

$$\text{For any } \mathcal{T}\in\{\mathrm{RS},\mathrm{SL},\mathrm{RL}\}\quad \min_{\theta_1\in I_1}\mathcal{T}^1(\theta_1)\le\mathcal{T}^2(\theta_2^{\min})\quad\text{and}\quad \min_{\theta_1\in I_1}\mathcal{T}^1(\theta_1)\le\mathcal{T}^2(\theta_2^{\max}) \tag{6}$$

Substituting for $\min_{\theta_1\in I_1}\mathrm{RSL}(\theta_1,\theta_2^{\min})$ and $\min_{\theta_1\in I_1}\mathrm{RSL}(\theta_1,\theta_2^{\max})$ in Eq. (3) using Eqs. (4) and (5) and simplifying further using Eq. (6), we get

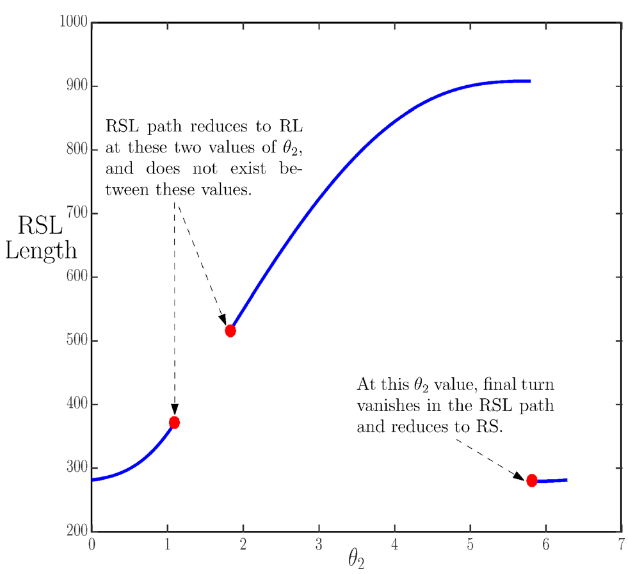

Fig. 5 Given θ_1, the length of the RSL path varies monotonically with respect to θ_2 wherever the path exists and none of its curved segments vanishes

$$\min_{\theta_1\in I_1}\min_{\theta_2\in I_2}\mathrm{RSL}(\theta_1,\theta_2) = \min\{\mathrm{RSL}^*,\min_{\theta_1\in I_1}\{\mathrm{RS}^1(\theta_1),\mathrm{SL}^1(\theta_1),\mathrm{RL}^1(\theta_1)\}\} \tag{7}$$

where

$$\begin{aligned}\mathrm{RSL}^* := \min\{&\mathrm{RSL}(\theta_1^{\min},\theta_2^{\min}),\mathrm{RSL}(\theta_1^{\max},\theta_2^{\min}),\\ &\mathrm{RSL}(\theta_1^{\min},\theta_2^{\max}),\mathrm{RSL}(\theta_1^{\max},\theta_2^{\max})\}\end{aligned} \tag{8}$$

As Lemma 4.1 is also applicable to RSR, LSL, and LSR paths, one can use the above procedure and simplify $\min_{\theta_1\in I_1,\theta_2\in I_2}\mathrm{RSR}(\theta_1,\theta_2)$, $\min_{\theta_1\in I_1,\theta_2\in I_2}\mathrm{LSL}(\theta_1,\theta_2)$, and $\min_{\theta_1\in I_1,\theta_2\in I_2}\mathrm{LSR}(\theta_1,\theta_2)$ in a similar way. Combining all these results, we obtain the following:

$$\begin{aligned}\min_{\theta_1\in I_1}\min_{\theta_2\in I_2}\min_{\mathcal{P}\in\{\mathrm{RSR,RSL,LSR,LSL}\}}\mathcal{P}(\theta_1,\theta_2) &= \min\{\mathcal{P}^*,\min_{\theta_1\in I_1}\{\mathrm{RS}^1(\theta_1),\mathrm{SR}^1(\theta_1),\mathrm{LS}^1(\theta_1),\mathrm{SL}^1(\theta_1),\\ &\quad \mathrm{LR}^1(\theta_1),\mathrm{RL}^1(\theta_1)\}\}\end{aligned} \tag{9}$$

where

$$\begin{aligned}\mathcal{P}^* := \min_{\mathcal{P}\in\{\mathrm{RSR,RSL,LSR,LSL}\}}\min\{&\mathcal{P}(\theta_1^{\min},\theta_2^{\min}),\mathcal{P}(\theta_1^{\max},\theta_2^{\min}),\\ &\mathcal{P}(\theta_1^{\min},\theta_2^{\max}),\mathcal{P}(\theta_1^{\max},\theta_2^{\max})\}.\end{aligned} \tag{10}$$

4.2 Optimizing RLR and LRL Paths. Goaoc et al. [28] have shown that the RLR and LRL paths cannot lead to an optimal Dubins path if the distance between the two targets is greater than 4ρ. Therefore, in this section, we assume that the distance between the two targets is at most 4ρ. We will focus on $\min_{\theta_1\in I_1,\theta_2\in I_2}\mathrm{LRL}(\theta_1,\theta_2)$; $\min_{\theta_1\in I_1,\theta_2\in I_2}\mathrm{RLR}(\theta_1,\theta_2)$ can be solved in a similar way. Given θ_1, unlike the length of the RSL path, $\mathrm{LRL}(\theta_1,\theta_2)$ is not monotonous with respect to θ_2 when LRL exists. Without loss of generality, we assume that $\theta_1=0$ and first aim to understand $\mathrm{LRL}(0,\theta_2)$ as a function of θ_2 (refer to Fig. 6). Target 1 is located at the origin, and target 2 is located at $(\bar{x},\bar{y})$. The angles α and β in Fig. 6 are functions of θ_2. For brevity, we use α and β in place of $\alpha(\theta_2)$ and $\beta(\theta_2)$, respectively. Let $\mathrm{LRL}(0,\theta_2)$ be denoted as $\mathfrak{D}(\theta_2) := (2\pi+2\alpha+2\beta+\theta_2)\rho$. In the ensuing discussion, we use the fact that the length of the *R* segment in an LRL path must be greater than $\pi\rho$ (i.e., $0<\alpha+\beta<\pi$) for the LRL path to be an optimal path between any two targets [23,29].

Lemma 4.2. *If the LRL path exists and none of its curved segments vanishes, then for any θ_2 such that $0<\alpha(\theta_2)+\beta(\theta_2)<\pi$, $d\mathfrak{D}/d\theta_2\neq 0$ except when $\mathfrak{D}(\theta_2)$ reaches a maximum, i.e., θ_2 satisfies $\alpha+\pi/2=\theta_2$.*

Proof. Using Fig. 6, α and β can be obtained in terms of θ_2 as follows:

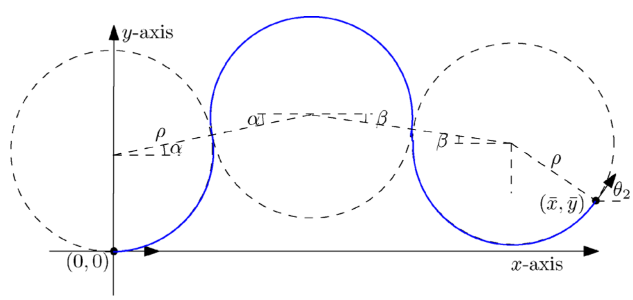

Fig. 6 LRL path for $\theta_1 = 0$

$$2\rho\sin\alpha + \rho = 2\rho\sin\beta + \rho\cos\theta_2 + \bar{y} \tag{11}$$

$$2\rho\cos\alpha + 2\rho\cos\beta + \rho\sin\theta_2 = \bar{x} \tag{12}$$

Differentiating and simplifying the above equations, we get

$$\cos\alpha\frac{d\alpha}{d\theta_2} - \cos\beta\frac{d\beta}{d\theta_2} = -\frac{\sin\theta_2}{2} \tag{13}$$

$$\sin\alpha\frac{d\alpha}{d\theta_2} + \sin\beta\frac{d\beta}{d\theta_2} = \frac{\cos\theta_2}{2} \tag{14}$$

Further solving for the derivatives, we get

$$\frac{d\beta}{d\theta_2} = \frac{\cos(\theta_2 - \alpha)}{2\sin(\alpha + \beta)} \tag{15}$$

$$\frac{d\alpha}{d\theta_2} = \frac{\cos(\theta_2 + \beta)}{2\sin(\alpha + \beta)} \tag{16}$$

Therefore,

$$\frac{d\mathfrak{D}}{d\theta_2} = \rho\left(2\frac{d\beta}{d\theta_2} + 2\frac{d\alpha}{d\theta_2} + 1\right) \tag{17}$$

$$= \rho\left(\frac{\cos(\theta_2 - \alpha)}{\sin(\alpha + \beta)} + \frac{\cos(\theta_2 + \beta)}{\sin(\alpha + \beta)} + 1\right) \tag{18}$$

Equation $d\mathfrak{D}/d\theta_2 = 0$ yields the following possibilities: $\theta_2 = \pi/2 + \alpha$ or $\theta_2 + \beta = -\pi/2$. $\theta_2 + \beta = -\pi/2$ corresponds to the case where the second left turn disappears; there is a jump in the length of the LRL path at this θ_2, and therefore, $d\mathfrak{D}/d\theta_2$ does not exist. $\theta_2 = \pi/2 + \alpha$ corresponds to the case where the turn angle in the right turn is equal to the turn angle in the second left turn; one can verify that $\mathfrak{D}(\theta_2)$ reaches a maximum at this point because $d^2\mathfrak{D}/d\theta_2^2 = -(3\rho/2)(1 + \cos(\alpha + \beta))/\sin(\alpha + \beta) < 0$ (refer to Fig. 7). □

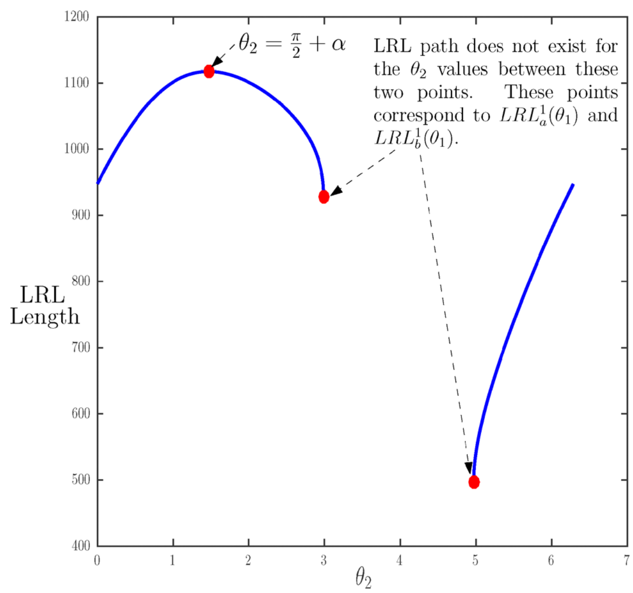

Fig. 7 Given θ_1, the length of the LRL path reaches a maximum when $\theta_2 = (\pi/2) + \alpha$, as shown. This figure also shows the values of θ_2 where the LRL path just ceases to exist.

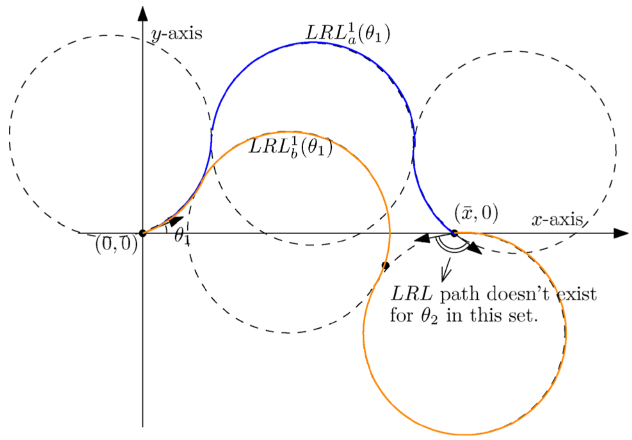

Fig. 8 Given θ_1, the LRL paths when the arc angle in the right turn is π. This figure shows the angles for θ_2 when the LRL path does not exist.

The derivatives of $\mathrm{LRL}(\theta_1, \theta_2)$ do not exist when any turn in the path disappears or when the angle in the right turn becomes equal to π, as shown in Fig. 8. The lengths of the two paths (Fig. 8) when the LRL path just ceases to exist are denoted by $\mathrm{LRL}_a^1(\theta_1)$ and $\mathrm{LRL}_b^1(\theta_1)$. Therefore, applying the above lemma to the LRL path and following similar steps to those in Sec. 4.1, we get the following result:

$$\begin{aligned}
&\min_{\theta_2 \in I_2}\{\mathrm{LRL}(\theta_1, \theta_2)\} \\
&:= \min\{\mathrm{LRL}(\theta_1, \theta_2^{\min}), \mathrm{LRL}(\theta_1, \theta_2^{\max}), \mathrm{LR}^1(\theta_1), \\
&\quad \mathrm{RL}^1(\theta_1), \mathrm{LRL}_a^1(\theta_1), \mathrm{LRL}_b^1(\theta_1)\}
\end{aligned} \tag{19}$$

Again, as in Sec. 4.1, one can further simplify the above optimization problem

$$\begin{aligned}
&\min_{\theta_1 \in I_1}\min_{\theta_2 \in I_2}\{\mathrm{LRL}(\theta_1, \theta_2)\} \\
&= \min\{\mathrm{LRL}^*, \min_{\theta_1 \in I_1}\{\mathrm{LR}^1(\theta_1), \mathrm{RL}^1(\theta_1), \mathrm{LRL}_a^1(\theta_1), \mathrm{LRL}_b^1(\theta_1)\}\}
\end{aligned} \tag{20}$$

where

$$\begin{aligned}
\mathrm{LRL}^* := \min\{&\mathrm{LRL}(\theta_1^{\min}, \theta_2^{\min}), \mathrm{LRL}(\theta_1^{\max}, \theta_2^{\min}), \\
&\mathrm{LRL}(\theta_1^{\min}, \theta_2^{\max}), \mathrm{LRL}(\theta_1^{\max}, \theta_2^{\max})\}.
\end{aligned}$$

Note that $\mathrm{LRL}_a^1(\theta_1)$ and $\mathrm{LRL}_b^1(\theta_1)$ can never result in an optimal path because the angle in the right turn is equal to π [29]. Therefore, once Eq. (20) is substituted in Eq. (1), the functions $\mathrm{LRL}_a^1(\theta_1)$ and $\mathrm{LRL}_b^1(\theta_1)$ will drop out.

$\min_{\theta_1 \in I_1}\min_{\theta_2 \in I_2}\{\mathrm{RLR}(\theta_1, \theta_2)\}$ can be simplified in a similar way. Hence, combining the above results with Eq. (9), we obtain the following result.

Theorem 4.1.

$$\min_{\theta_1 \in I_1} \min_{\theta_2 \in I_2} \{d_{12}(\theta_1, \theta_2)\} = \min\{d^*, \min_{\theta_1 \in I_1} \{\mathrm{RS}^1(\theta_1), \mathrm{SR}^1(\theta_1), \mathrm{LS}^1(\theta_1), \mathrm{SL}^1(\theta_1), \mathrm{LR}^1(\theta_1), \mathrm{RL}^1(\theta_1)\}\} \quad (21)$$

where

$$d^* := \min\{d_{12}(\theta_1^{\min}, \theta_2^{\min}), d_{12}(\theta_1^{\max}, \theta_2^{\min}), d_{12}(\theta_1^{\min}, \theta_2^{\max}), d_{12}(\theta_1^{\max}, \theta_2^{\max})\}.$$

The above theorem states that the optimum to the Dubins interval problem has to be either d^* (which is computed using standard Dubins paths with at most three segments where both the departure and the arrival angles belong to the boundary of the intervals) or the length of a Dubins path with at most two segments where either the departure or the arrival angle belongs to the boundary of the intervals. As we already know how to compute d^* [23], we will now provide algorithms to solve for the optimal Dubins paths with at most two segments (i.e., to solve $\min_{\theta_1 \in I_1} \mathcal{P}(\theta_1)$ for any path $\mathcal{P} \in \{\mathrm{RS}^1, \mathrm{SR}^1, \mathrm{LS}^1, \mathrm{SL}^1, \mathrm{LR}^1, \mathrm{RL}^1\}$). This will solve the Dubins interval problem.

5 Algorithms for Optimizing Dubins Paths With at Most Two Segments

In this section, we will first present algorithms to find the shortest RS path and the RL path: $\min_{\theta_1 \in I_1}\{\mathrm{RS}^1(\theta_1)\}$ and $\min_{\theta_1 \in I_1}\{\mathrm{RL}^1(\theta_1)\}$. These algorithms can then be used to solve $\min_{\theta_1 \in I_1} \mathcal{P}(\theta_1)$ for any $\mathcal{P} \in \{\mathrm{SR}^1, \mathrm{LS}^1, \mathrm{SL}^1, \mathrm{LR}^1\}$ using simple reflections of the points about the x or the y axis as discussed in Ref. [30]. For example, $\min_{\theta_1 \in I_1}\{\mathrm{LS}^1(\theta_1)\}$ can be solved by considering a reflection of the points about the x-axis as shown in Fig. 9.

5.1 Optimizing the RS Path. Without loss of generality, a reference frame can be chosen such that target 1 is at the origin and target 2 lies on the x-axis as shown in Fig. 10. Here $\bar{x}$ represents the Euclidean distance between the targets. Given θ_1, the existence of the RS path as well as its length can be determined using geometry. The length of the S path, the angle between the x-axis and the S path, and the final arrival angle at target 2 are also functions of θ_1 and can be expressed as $L(\theta_1)$, $\phi(\theta_1)$, and $\theta_2(\mathrm{RS}, \theta_1)$, respectively. Let the length of the RS path be denoted as $\mathfrak{D}(\theta_1)$. For brevity, in some places we will use L, ϕ, θ_2, and $\mathfrak{D}$ instead of $L(\theta_1), \phi(\theta_1), \theta_2(\mathrm{RS}, \theta_1)$, and $\mathfrak{D}(\theta_1)$, respectively. Let $d_S := \bar{x}$ if the angle of the straight line joining the two targets lies in the intervals I_1 and I_2. If the angle constraints are not satisfied, d_S is set to ∞. Similarly, let d_R denote the length of the shortest circular arc of type R that joins the two targets such that the boundary angles of the arc belong to the respective intervals at the targets. If such an arc does not exist, d_R is set to ∞. In the following lemma, we assume that $[\theta_1^{\min}, \theta_1^{\max}] \subseteq [0, 2\pi]$ and $[\theta_2^{\min}, \theta_2^{\max}] \subseteq [0, 2\pi]$.

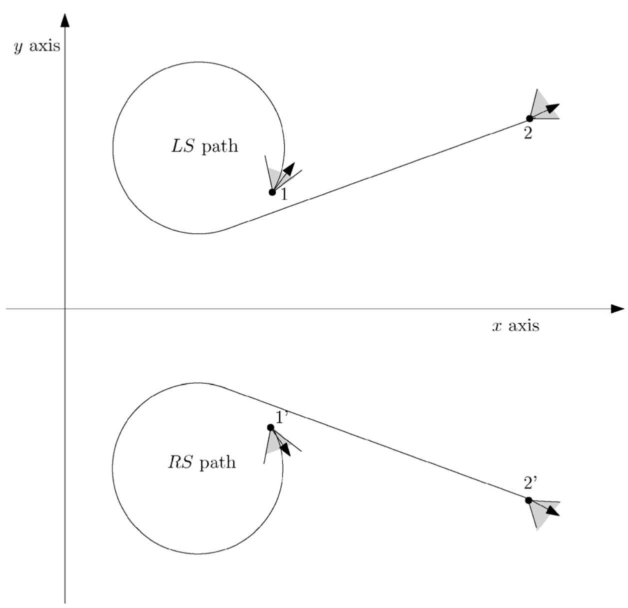

Fig. 9 One can solve $\min_{\theta_1 \in I_1}\{\mathrm{LS}^1(\theta_1)\}$ by considering the reflections of the points with respect to the x-axis and solving the corresponding $\min_{\theta_1 \in I_1}\{\mathrm{RS}^1(\theta_1)\}$

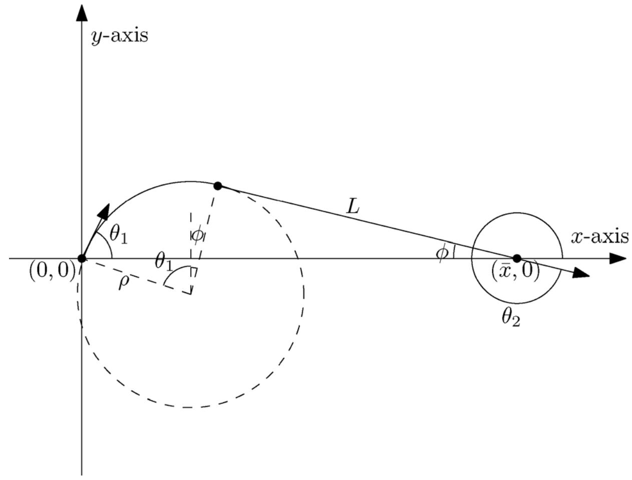

Fig. 10 RS path

Lemma 5.1. $\min_{\theta_1 \in I_1} \{\mathrm{RS}^1(\theta_1)\} = \min\{d_S, d_R, \mathrm{RS}^1(\theta_1^{\min}), \mathrm{RS}^2(\theta_2^{\min}), \mathrm{RS}^2(\theta_2^{\max})\}$.

Proof. Refer to the Appendix for the proof.

Following the above lemma, the algorithm to compute $\min_{\theta_1 \in I_1}\{\mathrm{RS}^1(\theta_1)\}$ requires one to find each of the values in the set $\{d_S, d_R, \mathrm{RS}^1(\theta_1^{\min}), \mathrm{RS}^2(\theta_2^{\min}), \mathrm{RS}^2(\theta_2^{\max})\}$ and select the least value.

5.2 Optimizing the RL Path. We use similar notations as in Sec. 5.1 (refer to Fig. 11). The angles $\phi(\theta_1)$ and $\theta_2(\mathrm{RL}, \theta_1)$ are

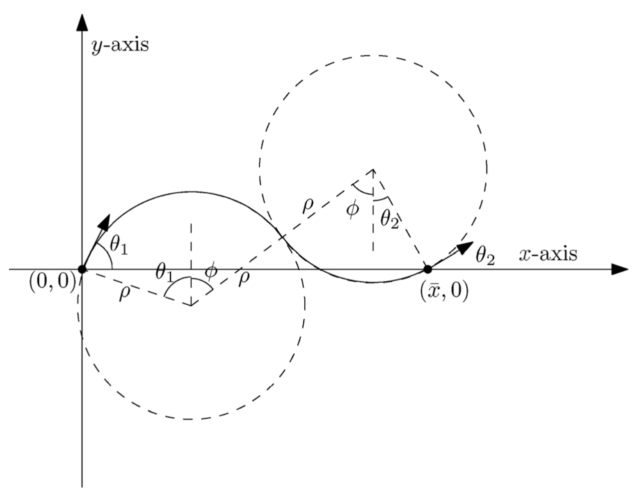

Fig. 11 RL path

also written as ϕ and θ_2, for brevity. The length of the RL path is denoted as $\mathfrak{D}(\theta_1)$ and is equal to $\rho(\theta_1 + \theta_2 + 2\phi)$. RL paths do not exist when $\bar{x} > 4\rho$. In addition, even when $0 \le \bar{x} \le 4\rho$, there are a subset of angles of θ_1 for which an RL path does not exist.

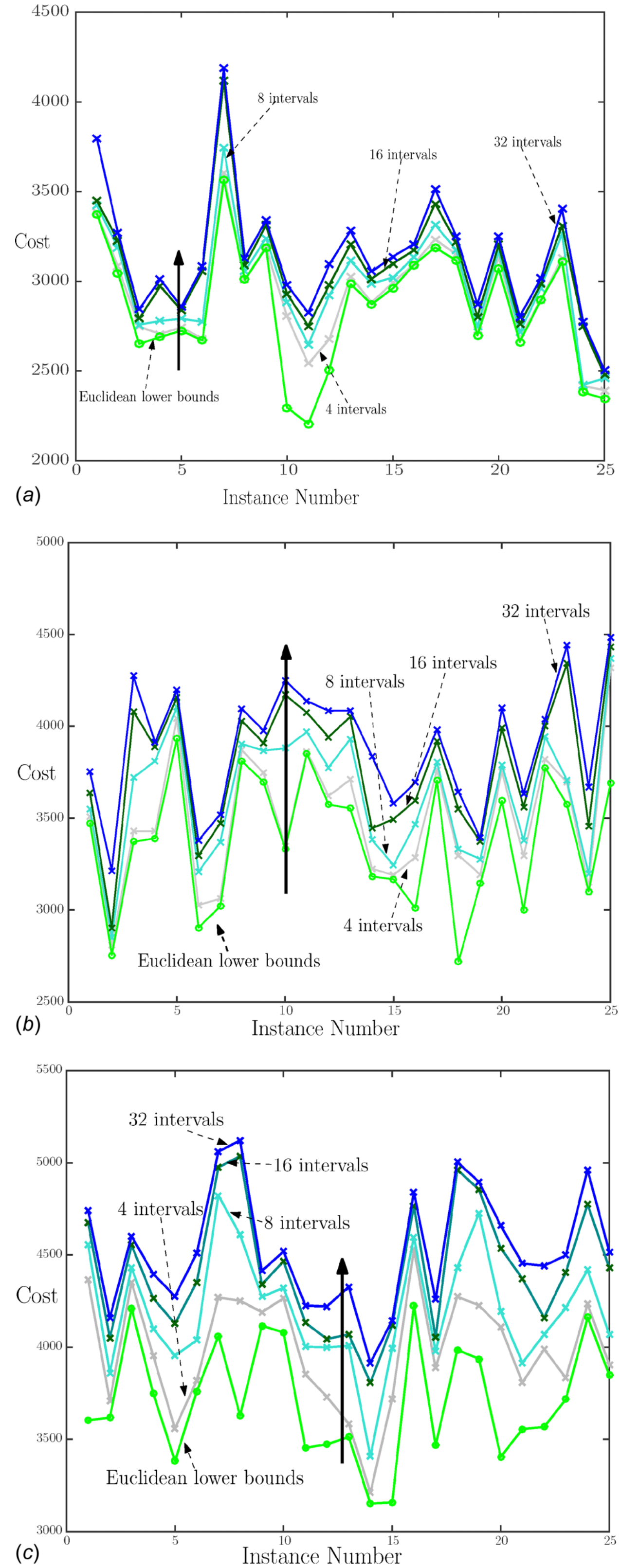

Fig. 12 Lower bounds computed with 4, 8, 16, and 32 intervals at each target for 25 instances: (*a*) 10 targets, (*b*) 15 targets, and (*c*) 20 targets

Moreover, given θ_1, there are two possible RL paths, as either $\phi + \theta_2 \le \pi$ or $\phi + \theta_2 > \pi$. In the following discussion and in Fig. 11, we assume that $\phi + \theta_2 < \pi$. The other RL path can be addressed similarly.

We first define some values of θ_1 where the optimum can occur (these correspond to the extreme values of $\mathfrak{D}$ and θ_2 for the RL path and will be derived later in the proof). Let θ^{1*} be the solution to the equation $\theta_2(\mathrm{RL}, \theta_1) = \theta_1$. Also, let θ^{2*} and θ^{3*} be the solutions to equation $\phi(\theta_1) + \theta_2(\mathrm{RL}, \theta_1) = \pi$. Let d_L denote the length of the shortest circular arc of type L that joins the two targets such that the boundary angles of the arc belong to the corresponding intervals at the targets and $\phi + \theta_2 < \pi$. If such an arc does not exist, then d_L is set to ∞. Let $RL^* = \min\{\mathrm{RL}^1(\theta_1^{\max}), \mathrm{RL}^1(\theta_1^{\min}), \mathrm{RL}^2(\theta_2^{\min}), \mathrm{RL}^2(\theta_2^{\max}\}$.

Lemma 5.2. *If* $\bar{x} > 2\rho$, $\min_{\theta_1 \in I_1}\{\mathrm{RL}^1(\theta_1)\} = \min\{\mathrm{RL}^1(\theta^{1*}), \mathrm{RL}^1(\theta^{2*}), \mathrm{RL}^1(\theta^{3*}), \mathrm{RL}^*\}$. *If* $0 \le \bar{x} \le 2\rho$, $\min_{\theta_1 \in I_1}\{\mathrm{RL}^1(\theta_1)\} = \min\{d_L, d_R, \mathrm{RL}^1(\theta^{1*}), \mathrm{RL}^*\}$.

Proof. Refer to the Appendix.

Following the above lemma, the algorithm to compute $\min_{\theta_1 \in I_1}\{\mathrm{RL}^1(\theta_1)\}$ requires one to find each of the values in the set $\{\mathrm{RL}^1(\theta^{1*}), \mathrm{RL}^1(\theta^{2*}), \mathrm{RL}^1(\theta^{3*}), \mathrm{RL}^*\}$ and select the least value.

In summary, the above algorithms can be used to compute the cost of traveling between the sectors in the lower bounding problem as stated in Sec. 2. The lower bounding problem is a one-in-a-set TSP. We use the Noon-Bean transformation [18,25] to first convert the one-in-a-set TSP into an ATSP. Then we use a transformation method outlined in Ref. [26] to convert the ATSP into a symmetric TSP. This method converts an asymmetric instance with n nodes into a symmetric instance with $3n$ nodes. We chose this method primarily because unlike other transformations, there is no big-M constant involved, and therefore, we did not have any numerical difficulties such as those faced in Refs. [18], [21], and [22]. For example, the transformed TSP instance corresponding to 20 targets with 32 discretizations at each target has 1920 nodes. Each of the transformed TSP instances was solved to optimality using the Concorde solver [27].

6 Numerical Results

Computational results are presented for 25 instances with 10, 15, and 20[3] targets in each instance. The locations of the targets were uniformly sampled from a 1000×1000 square. The minimum turning radius of the vehicle was chosen to be 100. The heading angles at each target are discretized into 4, 8, 16, and 32 intervals. The improvement of the lower bounds as the number of discretizations or intervals increases is shown in Fig. 12. On average, the improvement of the lower bounds with respective to the optimal ETSP cost for 32 intervals was 22.28%.

A feasible solution is obtained by discretizing the angles at each target (32 values) and applying the transformation procedure similar to the lower bound computation. The comparison of the cost of the feasible solution with respect to the optimal Euclidean TSP cost and the lower bound (corresponding to 32 intervals at each target) for the 25 instances in each case is shown in Fig. 13. The average deviation of the cost of the feasible solution from its corresponding lower bound for all the instances is 5.2%, while the average deviation of the cost of the feasible solution from its corresponding ETSP cost is 29.2%. In one of the instances, we found the cost of the feasible solution from its corresponding lower bound improved by approximately 44%. These results show that the proposed approach can be used to obtain tight lower bounds for the DTSP. A feasible DTSP solution and an optimal solution corresponding to the lower bound for an instance are shown in Fig. 14.

We have also tested the algorithms by varying the minimum turning radius (ρ) of the vehicle. The lower bounding algorithm is

[3]These 25 instances each with 20 targets are the same instances used in Fig. 2.

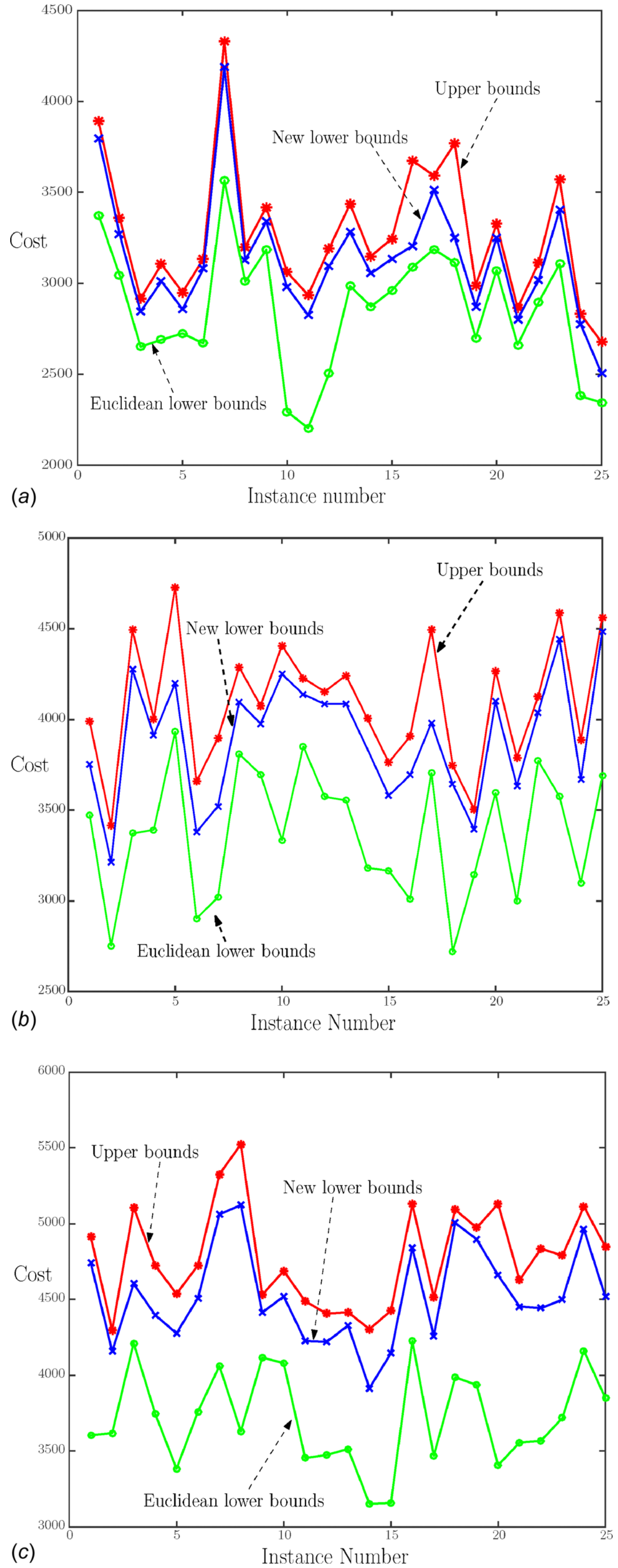

Fig. 13 Comparison between lower bounds and upper bounds for 32 discretizations, along with the optimal Euclidean TSP cost: (*a*) 10 targets, (*b*) 15 targets, and (*c*) 20 targets

run on the instances in Fig. 2 with four different values of $\rho \in \{50, 100, 150, 200\}$. The average of the lower and upper bounds for each case with 16 discretizations at each target is reported in Table 1. The first column of the table refers to the problem size or the number of targets, and the second columns refers to the minimum turning radius of the vehicle. The mean values over 25 instances for the upper bounds, lower bounds (computed using our algorithm), and the Euclidean lower bounds are listed in the third, the fourth, and the fifth columns. The last two columns denote the mean of the ratio of upper and lower bounds. The gap between the Euclidean lower bounds and upper bounds are higher for larger minimum turn radii, which is expected. The proposed approach significantly improved the bounds for problem instances with a turning radius equal to 150 and 200 units. For example, in the case of 20 targets with $\rho = 200$, the ratio $(\mathrm{UB}/\mathrm{LB})$ is trimmed to 1.25 from 1.98, which is significant. This improvement in the ratio using the new lower bounds compared to the Euclidean lower bounds indicates the effectiveness of using our proposed approach.

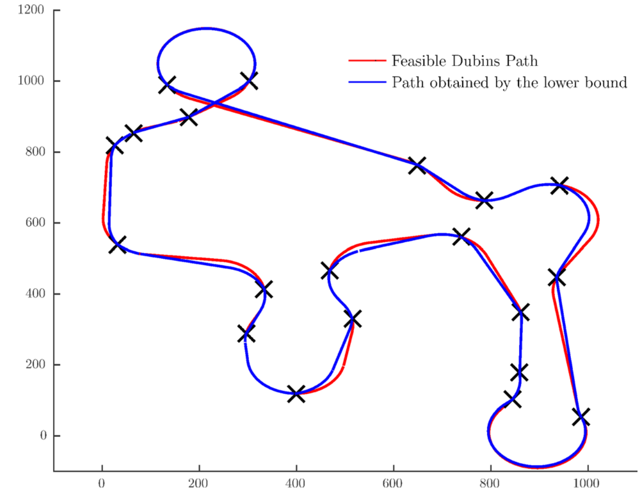

Fig. 14 A feasible Dubins path for an instance with 20 targets and the path obtained from lower bound computation

We have also analyzed the results to find out the average number of two segment or three segment Dubins paths in an optimal solution to the lower bounding problem. Specifically, given an instance and its corresponding optimal solution, we compute the proportion of the number of Dubins paths with at most two segments or three segments in the optimal solution. Similarly, we also compute the proportion of costs contributed by the Dubins paths with at most two segments or three segments in an optimal solution. The mean values of these results over 25 instances for varying number of sectors at each target are shown in Table 2. These results indicate a generic trend we observed in all our simulations: when the number of discretizations increases, the solutions to the Dubins interval problem have three segments and tend to have both the arrival and the departure angles of the solutions occur at the boundaries of the sectors. We also fixed the number of discretizations at 16 and varied the minimum turning radius of the vehicle to find any pattern in the contributions of the two segment or three segment paths. Table 3 shows these results. As noted, we did not observe any specific pattern when the minimum turning radius was changed.

7 Conclusion

We provide a systematic procedure to find lower bounds for the DTSP. This paper provides a new direction for developing approximation algorithms for the DTSP. Currently, the transformation method increases the size of the one-in-a-set TSP by two or three times, resulting in a large TSP. Computationally, more efficient tools for directly solving the one-in-a-set TSP will be useful in finding tighter lower and upper bounds for the DTSP. Future work can also address the same problem with multiple vehicles and other precedence constraints.

Table 1 Results for varying minimum turning radius (ρ) of the vehicle

No. of targets	ρ	Upper bound (UB)	Lower bound (LB)	Euclidean bound (EB)	Ratio (UB/LB)	Ratio (UB/EB)
10	50	2964.24	2909.44	2851.60	1.02	1.04
10	100	3325.20	3077.56	2851.60	1.08	1.17
10	150	3905.80	3438.08	2851.60	1.14	1.37
10	200	4670.56	3957.32	2851.60	1.19	1.65
15	50	3602.24	3471.92	3373.08	1.04	1.07
15	100	4234.36	3790.80	3373.08	1.12	1.26
15	150	5091.80	4350.76	3373.08	1.18	1.52
15	200	5945.44	4888.24	3373.08	1.22	1.78
20	50	4040.04	3843.04	3713.44	1.05	1.09
20	100	4977.96	4413.32	3713.44	1.13	1.35
20	150	6181.44	5223.00	3713.44	1.19	1.67
20	200	7313.52	5854.36	3713.44	1.25	1.98

Note: The bounds and ratios indicate mean values for 25 instances.

Table 2 Average contributions from two segment or three segment Dubins paths in an optimal solution to the lower bounding problem: results for different number of sectors at each target

		Average proportion of Dubins paths		Average cost proportion of Dubins paths	
No. of targets	No. of sectors	With $\leq$2 segments	With three segments	With $\leq$2 segments	With three segments
10	4	0.816	0.184	0.8119	0.1881
10	8	0.564	0.436	0.4817	0.5182
10	16	0.292	0.708	0.2123	0.7877
10	32	0.172	0.828	0.1336	0.8664
15	4	0.8346	0.1653	0.7927	0.2073
15	8	0.6053	0.3947	0.537	0.463
15	16	0.3626	0.6373	0.2929	0.7071
15	32	0.1973	0.8027	0.1585	0.8415
20	4	0.864	0.136	0.822	0.178
20	8	0.66	0.34	0.554	0.4459
20	16	0.398	0.602	0.338	0.662
20	32	0.246	0.754	0.1958	0.8043

Table 3 Average contributions from two segment or three segment Dubins paths in an optimal solution to the lower bounding problem: results for varying minimum turning radius of the vehicle

		Average proportion of Dubins paths		Average cost proportion of Dubins paths	
No. of targets	ρ	With $\leq$2 segments	With three segments	With $\leq$2 segments	With three segments
10	50	0.264	0.736	0.2201	0.78
10	100	0.292	0.708	0.2123	0.7877
10	150	0.36	0.64	0.2769	0.7231
10	200	0.432	0.568	0.3459	0.6541
15	50	0.2747	0.7253	0.2445	0.7554
15	100	0.3626	0.6373	0.2929	0.7071
15	150	0.4267	0.5733	0.3313	0.6687
15	200	0.4746	0.5253	0.3539	0.6462
20	50	0.284	0.716	0.2288	0.7712
20	100	0.398	0.602	0.338	0.662
20	150	0.48	0.52	0.3703	0.6297
20	200	0.51	0.49	0.3678	0.6322

Appendix

A.1 Proof of Lemma 5.1. Using Fig. 10, one can relate L and ϕ to θ_1 using the following equations:

$$\begin{aligned}\rho\sin\phi + L\cos\phi &= \bar{x} - \rho\sin\theta_1\\ \rho\cos\phi - L\sin\phi &= \rho\cos\theta_1\end{aligned} \tag{A1}$$

The arrival angle $\theta_2(\mathrm{RS},\theta_1)$ at target 2 is equal to $2\pi - \phi$. We now consider two different cases: $\bar{x} > 2\rho$ and $\bar{x} \leq 2\rho$ (the RS path does not exist for a subset of angles of θ_1 if $\bar{x} < 2\rho$).

Case 1: $\bar{x} > 2\rho$.

The length of the RS path is $\mathfrak{D} := (\theta_1 + \phi)\rho + L$. Therefore, $d\mathfrak{D}/d\theta_1 := (1 + d\phi/d\theta_1)\rho + dL/d\theta_1$. The derivatives of ϕ and L with respect to θ_1 can be obtained by differentiating Eq. (A1) as follows:

$$(\rho\cos\phi - L\sin\phi)\frac{d\phi}{d\theta_1} + \cos\phi\frac{dL}{d\theta_1} = -\rho\cos\theta_1 \tag{A2}$$

$$-(\rho\sin\phi + L\cos\phi)\frac{d\phi}{d\theta_1} - \sin\phi\frac{dL}{d\theta_1} = -\rho\sin\theta_1 \tag{A3}$$

Solving these equations and simplifying further, we obtain the following:

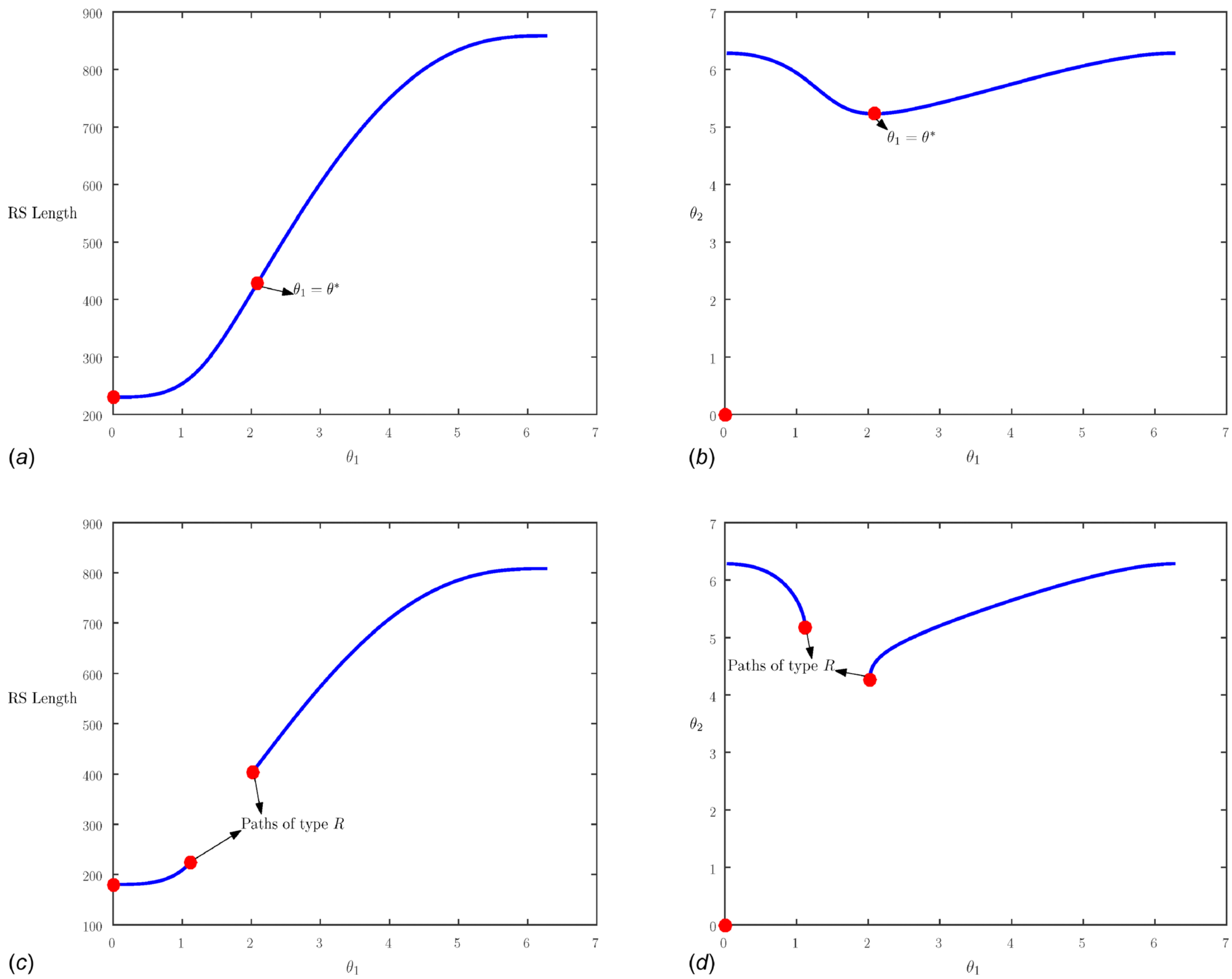

Fig. 15 RS path: examples illustrating $\mathfrak{D}(\theta_1)$ and $\theta_2(\mathrm{RS}, \theta_1)$: (a) $\bar{x} > 2\rho$, (b) $\bar{x} > 2\rho$, (c) $\bar{x} \le 2\rho$, and (d) $\bar{x} \le 2\rho$

$$\frac{d\phi}{d\theta_1} = \frac{\bar{x}}{L}\cos\phi - 1 \tag{A4}$$

$$\frac{dL}{d\theta_1} = -\frac{\rho\bar{x}}{L}\cos\theta_1 \tag{A5}$$

Therefore,

$$\frac{d\mathfrak{D}}{d\theta_1} = \left(1 + \frac{d\phi}{d\theta_1}\right)\rho + \frac{dL}{d\theta_1} \tag{A6}$$

$$= \frac{\bar{x}}{L}(\rho\cos\phi - \rho\cos\theta_1) \tag{A7}$$

$$= \bar{x}\sin\phi \tag{A8}$$

For any $\theta_1 \in [0, 2\pi]$, it is easy to verify geometrically that $\phi \in [0, \pi]$ using Fig. 10. Therefore, $\forall \theta_1 \in (0, 2\pi)$, $d\mathfrak{D}/d\theta_1 > 0$, i.e., the length of the RS path increases monotonically from $\bar{x}$. When $\theta_1 = 2\pi$, the curved segment in the RS path vanishes and the length of the RS path returns to the Euclidean distance between the targets ($\bar{x}$). Even though the length of the RS path increases monotonically for any $\theta_1 \in [0, 2\pi)$, the arrival angle at target 2, $\theta_2 := 2\pi - \phi$, first decreases with θ_1, reaches a minimum at some $\theta_1 = \theta^*$, and increases to 2π. This minimum can be computed by solving $d\phi/d\theta_1 = 0 \Rightarrow (\bar{x}/L)\cos(\phi(\theta^*)) - 1 = 0$ or $\cos(\phi(\theta^*)) = L/\bar{x}$. One can verify that at $\theta_1 = \theta^*$, θ_2 reaches a minimum.

Now, the optimum for $\min_{\theta_1 \in I_1}\{\mathrm{RS}^1(\theta_1)\}$ must satisfy one of the following conditions:

(1) $d\mathfrak{D}/d\theta_1 = 0$ or $\theta_1 = 0$ ($d\mathfrak{D}/d\theta_1$ does not exist at this point) or $\theta_1 = \theta_1^{\min}$ or $\theta_1 = \theta_1^{\max}$. $\forall \theta_1 \in (0, 2\pi)$, $d\mathfrak{D}/d\theta_1 \neq 0$. As the length of the RS path increases monotonically with respect to θ_1, we need not consider $\theta_1 = \theta_1^{\max}$. Therefore, for this condition, the optimum occurs when $\theta_1 = 0$ or $\theta_1 = \theta_1^{\min}$.

(2) $\theta_2 = \theta_2^{\min}$ or $\theta_2 = \theta_2^{\max}$.

Therefore, when $\bar{x} > 2\rho$, $\min_{\theta_1 \in I_1}\{\mathrm{RS}^1(\theta_1)\} := \min\{d_S, \mathrm{RS}^1(\theta_1^{\min}), \mathrm{RS}^2(\theta_2^{\min}), \mathrm{RS}^2(\theta_2^{\max})\}$.

Case 2: $\bar{x} \le 2\rho$.

In this case, the RS path is not defined for any $\theta_1 \in (\sin(\bar{x}/2\rho), \pi/2 + \cos(\bar{x}/2\rho))$. Moreover, when $\theta_1 = \sin(\bar{x}/2\rho)$ or $\theta_1 = \pi/2 + \cos(\bar{x}/2\rho)$, the RS path reduces to just one segment of type R. Therefore, following the same analysis as in the previous case, $\min_{\theta_1 \in I_1}\{\mathrm{RS}^1(\theta_1)\} := \min\{d_S, d_R, \mathrm{RS}^1(\theta_1^{\min}), \mathrm{RS}^2(\theta_2^{\min}), \mathrm{RS}^2(\theta_2^{\max})\}$. Hence this case is proved (Fig. 15).

A.2 Proof of Lemma 5.2. We can solve for ϕ and θ_2 using the following equations (Fig. 11):

$$\begin{aligned} 2\rho\cos\phi - \rho\cos\theta_2 &= \rho\cos\theta_1 \\ 2\rho\sin\phi + \rho\sin\theta_2 &= \bar{x} - \rho\sin\theta_1 \end{aligned} \tag{A9}$$

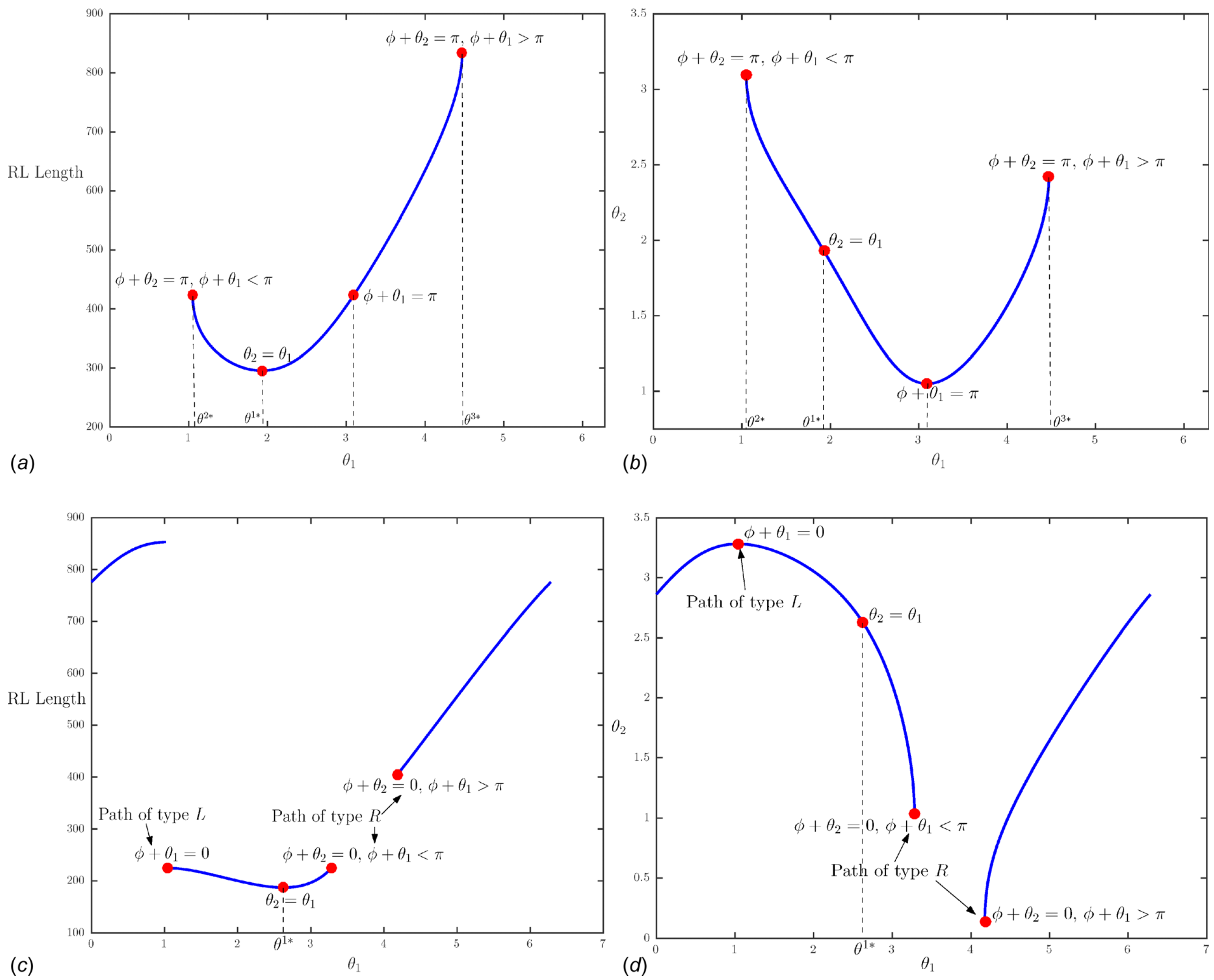

Fig. 16 RL path: examples illustrating $\mathfrak{D}(\theta_1)$ and $\theta_2(\mathrm{RL},\theta_1)$ for the case when $0\le\phi+\theta_2\le\pi$: (*a*) $\bar{x}>2\rho$, (*b*) $\bar{x}>2\rho$, (*c*) $\bar{x}\le2\rho$, and (*d*) $\bar{x}\le2\rho$

Differentiating and simplifying these equations, we get

$$-2\sin\phi\frac{d\phi}{d\theta_1}+\sin\theta_2\frac{d\theta_2}{d\theta_1}=-\sin\theta_1 \tag{A10}$$

$$2\cos\phi\frac{d\phi}{d\theta_1}+\cos\theta_2\frac{d\theta_2}{d\theta_1}=-\cos\theta_1 \tag{A11}$$

Solving further for $d\phi/d\theta_1$ and $d\theta_2/d\theta_1$, we get

$$\frac{d\phi}{d\theta_1}=\frac{\sin(\theta_1-\theta_2)}{2\sin(\phi+\theta_2)} \tag{A12}$$

$$\frac{d\theta_2}{d\theta_1}=-\frac{\sin(\theta_1+\phi)}{\sin(\phi+\theta_2)} \tag{A13}$$

$$\begin{aligned}\frac{d\mathfrak{D}}{d\theta_1}&=\rho\left(1+\frac{d\theta_2}{d\theta_1}+2\frac{d\phi}{d\theta_1}\right)\\&=\rho\left(1-\frac{\sin(\theta_1+\phi)}{\sin(\phi+\theta_2)}+\frac{\sin(\theta_1-\theta_2)}{\sin(\phi+\theta_2)}\right)\end{aligned} \tag{A14}$$

Equating $d\mathfrak{D}/d\theta_1=0$ and simplifying the equations, we get either $\phi+\theta_1=0$ or $\phi+\theta_2=0$ or $\theta_1=\theta_2$. $\phi+\theta_1=0$ or $\phi+\theta_2=0$ would imply that one of the circles vanishes; however, this is possible only when $\bar{x}\le2\rho$. When $\theta_1=\theta_2$, we note that $d\theta_2/d\theta_1=-1$ and $d\phi/d\theta_1=0$. Using this, one can verify that $d^2\mathfrak{D}/d\theta_1^2=2(1-\cos\theta_1+\phi))/\sin(\theta_1+\phi)\Rightarrow d^2\mathfrak{D}/d\theta_1^2>0$. Therefore, the length of the RL path reaches a minimum when $\theta_1=\theta_2$.

Case 1: $4\rho\ge\bar{x}\ge2\rho$.

The optimum for $\min_{\theta_1\in I_1}\{\mathrm{RL}^1(\theta_1)\}$ must occur at one of the extreme values of $\mathfrak{D}(\theta_1)$ or when $\theta_1\in\{\theta_1^{\min},\theta_1^{\max}\}$ or $\theta_2\in\{\theta_2^{\min},\theta_2^{\max}\}$. $\mathfrak{D}(\theta_1)$ reaches a local minimum at $\theta_1=\theta^{1*}$ (Fig. 16). Also, the RL path just ceases to exist when $\theta_1=\theta^{2*}$ or $\theta_1=\theta^{3*}$. Specifically, for a small $\varepsilon>0$, the RL path does not exist when $\theta_1=\theta^{2*}-\varepsilon$ or $\theta_1=\theta^{3*}+\varepsilon$. Therefore, $\min_{\theta_1\in I_1}\{\mathrm{RL}^1(\theta_1)\}:=\min\{\mathrm{RL}^1(\theta^{1*}),\mathrm{RL}^1(\theta^{2*}),\mathrm{RL}^1(\theta^{3*}),\mathrm{RL}^*\}$.

Case 2: $2\rho\ge\bar{x}\ge0$.

In this case, one of the circles may cease to exist, and therefore, the optimum may be equal to d_L or d_R if the corresponding angle constraints are met. Following the same arguments as in the previous case, we obtain $\min_{\theta_1\in I_1}\{\mathrm{RL}^1(\theta_1)\}:=\min\{d_L,d_R,\mathrm{RL}^1(\theta^{1*}),\mathrm{RL}^*\}$. Hence this case is proved.

References

[1] Rathinam, S., Sengupta, R., and Darbha, S., 2007, "A Resource Allocation Algorithm for Multivehicle Systems With Nonholonomic Constraints," IEEE Trans. Autom. Sci. Eng., **4**(1), pp. 98–104.

[2] Le Ny, J., Feron, E., and Frazzoli, E., 2012, "On the Dubins Traveling Salesman Problem," IEEE Trans. Autom. Control, **57**(1), pp. 265–270.

[3] Chandler, P., and Pachter, M., 1998, "Research Issues in Autonomous Control of Tactical UAVS," American Control Conference (ACC), Philadelphia, PA, June 24–26, pp. 394–398.

[4] Medeiros, A. C., and Urrutia, S., 2010, "Discrete Optimization Methods to Determine Trajectories for Dubins' Vehicles," Electron. Notes Discrete Math., **36**, pp. 17–24.

[5] Macharet, D., and Campos, M., 2014, "An Orientation Assignment Heuristic to the Dubins Traveling Salesman Problem," Advances in Artificial Intelligence—IBERAMIA 2014, Santiago de Chile, Chile, Nov. 24–27, pp. 457–468.

[6] Macharet, D. G., Alves Neto, A., da Camara Neto, V. F., and Campos, M. F., 2013, "Efficient Target Visiting Path Planning for Multiple Vehicles With Bounded Curvature," IEEE/RSJ International Conference on Intelligent Robots and Systems (IROS), Tokyo, Japan, Nov. 3–7, pp. 3830–3836.

[7] Macharet, D. G., Neto, A. A., da Camara Neto, V. F., and Campos, M. F., 2012, "Data Gathering Tour Optimization for Dubins' Vehicles," 2012 IEEE Congress on Evolutionary Computation (CEC), Brisbane, Australia, June 10–15, pp. 1–8.

[8] Sujit, P., Hudzietz, B., and Saripalli, S., 2013, "Route Planning for Angle Constrained Terrain Mapping Using an Unmanned Aerial Vehicle," J. Intell. Rob. Syst., **69**(1–4), pp. 273–283.

[9] Kenefic, R. J., 2008, "Finding Good Dubins Tours for UAVS Using Particle Swarm Optimization," J. Aerosp. Comput. Inf. Commun., **5**(2), pp. 47–56.

[10] Macharet, D. G., Neto, A. A., da Camara Neto, V. F., and Campos, M. F., 2011, "Nonholonomic Path Planning Optimization for Dubins' Vehicles," IEEE International Conference on Robotics and Automation (ICRA), Shanghai, China, May 9–13, pp. 4208–4213.

[11] Tang, Z., and Ozguner, U., 2005, "Motion Planning for Multitarget Surveillance With Mobile Sensor Agents," IEEE Trans. Rob., **21**(5), pp. 898–908.

[12] Savla, K., Frazzoli, E., and Bullo, F., 2008, "Traveling Salesperson Problems for the Dubins Vehicle," IEEE Trans. Autom. Control, **53**(6), pp. 1378–1391.

[13] Epstein, C., Cohen, I., and Shima, T., 2017, "On the Discretized Dubins Traveling Salesman Problem," IISE Trans., **49**(2), pp. 238–254.

[14] Ma, X., and Castañón, D., 2006, "Receding Horizon Planning for Dubins Traveling Salesman Problems," 45th IEEE Conference on Decision and Control (CDC), San Diego, CA, Dec. 13–15, pp. 5453–5458.

[15] Isaacs, J. T., and Hespanha, J. P., 2013, "Dubins Traveling Salesman Problem With Neighborhoods: A Graph-Based Approach," Algorithms, **6**(1), pp. 84–99.

[16] Anderson, R. P., and Milutinovic, D., 2014, "On the Construction of Minimum-Time Tours for a Dubins Vehicle in the Presence of Uncertainties," ASME J. Dyn. Syst. Meas. Control, **137**(3), p. 031001.

[17] Isaiah, P., and Shima, T., 2015, "Motion Planning Algorithms for the Dubins Travelling Salesperson Problem," Automatica, **53**, pp. 247–255.

[18] Oberlin, P., Rathinam, S., and Darbha, S., 2010, "Today's Traveling Salesman Problem," IEEE Rob. Autom. Mag., **17**(4), pp. 70–77.

[19] Manyam, S. G., Rathinam, S., Darbha, S., and Obermeyer, K. J., 2015, "Lower Bounds for a Vehicle Routing Problem With Motion Constraints," Int. J. Rob. Autom., **30**(3).

[20] Manyam, S. G., Rathinam, S., and Darbha, S., 2015, "Computation of Lower Bounds for a Multiple Depot, Multiple Vehicle Routing Problem With Motion Constraints," ASME J. Dyn. Syst. Meas. Control, **137**(9), p. 094501.

[21] Manyam, S. G., Rathinam, S., Darbha, S., and Obermeyer, K. J., 2012, "Computation of a Lower Bound for a Vehicle Routing Problem With Motion Constraints," ASME Paper No. DSCC2012-MOVIC2012-8713.

[22] Manyam, S. G., Rathinam, S., and Darbha, S., 2013, "Computation of Lower Bounds for a Multiple Depot, Multiple Vehicle Routing Problem With Motion Constraints," IEEE 52nd Annual Conference on Decision and Control (CDC), Florence, Italy, Dec. 10–13, pp. 2378–2383.

[23] Dubins, L. E., 1957, "On Curves of Minimal Length With a Constraint on Average Curvature, and With Prescribed Initial and Terminal Positions and Tangents," Am. J. Math., **79**(3), pp. 497–516.

[24] Manyam, S. G., Rathinam, S., Casbeer, D., and Garcia, E., 2017, "Tightly Bounding the Shortest Dubins Paths Through a Sequence of Points," J. Intell. Rob. Syst., **88**(2–4), pp. 495–511.

[25] Noon, C. E., and Bean, J. C., 1991, "A Lagrangian Based Approach for the Asymmetric Generalized Traveling Salesman Problem," Oper. Res., **39**(4), pp. 623–632.

[26] Gutin, G., and Punnen, A. P., eds., 2002, *The Traveling Salesman Problem and Its Variations* (Combinatorial Optimization), Kluwer Academic, Dordrecht, The Netherlands.

[27] Applegate, D. L., Bixby, R. E., Chvatal, V., and Cook, W. J., 2007, *The Traveling Salesman Problem: A Computational Study* (Princeton Series in Applied Mathematics), Princeton University Press, Princeton, NJ.

[28] Goaoc, X., Kim, H.-S., and Lazard, S., 2013, "Bounded-Curvature Shortest Paths Through a Sequence of Points Using Convex Optimization," SIAM J. Comput., **42**(2), pp. 662–684.

[29] Boissonnat, J.-D., Crzo, A., and Leblond, J., 1994, "Shortest Paths of Bounded Curvature in the Plane," J. Intell. Rob. Syst., **11**(1–2), pp. 5–20.

[30] Boissonnat, J.-D., and Bui, X.-N., 1994, "Accessibility Region for a Car That Only Moves Forwards Along Optimal Paths," INRIA, Saclay, France, Research Report No. 2181.